

王坤阳, 杜谷, 王冠, 等. 利用原子力显微镜研究致密砂岩储层黏土矿物形貌特征[J]. 岩矿测试, 2025, 44(2): 245–253. DOI: [10.15898/j.ykcs.202404040075](https://doi.org/10.15898/j.ykcs.202404040075).

WANG Kunyang, DU Gu, WANG Guan, et al. The Morphological Characteristics of Clay Minerals in a Tight Sandstone Reservoir by Atomic Force Microscopy[J]. Rock and Mineral Analysis, 2025, 44(2): 245–253. DOI: [10.15898/j.ykcs.202404040075](https://doi.org/10.15898/j.ykcs.202404040075).

利用原子力显微镜研究致密砂岩储层黏土矿物形貌特征

王坤阳*, 杜谷, 王冠, 何佳乐

(中国地质调查局成都地质调查中心, 四川 成都 610081)

摘要: 致密砂岩气作为非常规油气资源的重要组成部分, 对其储层矿物学特征的研究一直以来都是非常规油气领域研究热点。黏土矿物作为致密砂岩储层的主要组成矿物之一, 目前对其形貌特征的研究主要依赖于电子显微术, 但受其表面电荷吸附性及样品表面导电膜二次改造的影响, 很难对其表面形貌特征进行准确的精细刻画。然而, 致密砂岩储层主体孔径在 20~500nm, 伊蒙混层黏土、绿泥石、伊利石等黏土矿物为纳米孔隙发育的主要矿物之一, 随着致密砂岩储层微纳米孔隙系统的研究深入, 黏土矿物纳米形貌特征的研究对于致密砂岩储层评价显得愈发重要, 因此, 对黏土矿物纳米/亚纳米形貌特征的研究对于储层评价具有重要的意义。本文利用原子力显微镜(AFM)观察到川西须家河组致密砂岩晚成岩阶段中伊蒙混层黏土矿物发育平行阶梯条纹, 阶梯的两面凹角处形成了大量的纳米孔隙, 是无机纳米孔隙的主要组成部分; 绿泥石主要呈面平棱直的理想晶体生长形态, 生长层在纵向上有规律地无隙叠置, 晶体处于一个稳定的状态; 伊利石发育平行阶梯条纹或波纹状阶梯, 晶体形态不规则, 处于亚稳定状态。其次, 川西须家河组晚成岩阶段的黏土矿物构造背景相似、经历的成岩演化序列相同, 但是通过 AFM 观察到川西须家河组晚成岩阶段不同种类黏土矿物晶体形态各异、晶面阶梯发育程度不尽相同, 表明黏土矿物的形貌特征与成岩作用之间存在着空间耦合关系。

关键词: 原子力显微镜; 致密砂岩; 伊蒙混层黏土; 绿泥石; 伊利石; 生长阶梯; 川西须家河组

要点:

- (1) 原子力显微镜(AFM)克服了黏土矿物表面电荷的影响, 精细刻画了黏土矿物表面纳米/亚纳米形貌特征, 是一种有效的微区形貌观察方法。
- (2) 川西须家河致密砂岩中黏土矿物表面发育晶面台阶, 是纳米孔隙的主要组成部分。
- (3) 同一成岩阶段不同黏土矿物生长层厚度不同, 与成岩作用之间存在空间耦合关系。

中图分类号: P575.9; P618.13

文献标识码: A

致密砂岩气作为三大非常规油气资源之一, 是常规油气资源的主要接替者, 该类储层中 20~500nm 是油气聚集的主要场所, 而黏土矿物涵盖了所有小于 2μm 的铝硅酸盐矿物, 常见的有绿泥石、伊利石、蒙脱石及混层黏土等, 是致密砂岩储层主要的组成矿物之一, 该类矿物表面发育大量的纳米孔隙, 对其形貌特征进行精细刻画, 不仅可建立不

同成岩阶段与黏土矿物形貌特征的对应关系, 还可追踪晶体生长过程中温度、杂质及原子行为对晶体微形貌特征产生的影响^[1-3], 为成岩环境、储层评价的研究提供依据, 具有重要的研究意义。

目前用于表征矿物表面纳米形貌特征研究的核心方法主要有电子显微术、超分辨光学显微术与扫描探针显微术^[4-6]。电子显微术作为一种主要的微

收稿日期: 2024-04-04; 修回日期: 2024-09-04; 接受日期: 2024-09-06; 网络出版日期: 2024-10-21

基金项目: 国家自然基金青年科学基金项目“华南奥陶—志留纪之交氮循环及古海洋启示”(42102142)

第一作者: 王坤阳, 硕士, 高级工程师, 主要从事矿物微区分析。E-mail: wnagkunyang_1213@163.com。

通信作者: 杜谷, 硕士, 教授级高级工程师, 主要从事岩矿分析。E-mail: dugucgs@163.com。

区形貌观测手段,可对微米/纳米尺度的结构进行定性表征,运用该方法可观察到高岭石、伊利石等黏土矿物的形态特征^[7],在成岩历史恢复^[8]、热液蚀变研究、结晶习性^[9-10]、油气生成^[11]、运移及聚集等的研究中起着关键性作用然而该方法主要是在二维平面对矿物形貌进行定性表征,无法对显微结构进行定量分析。此外,该方法受样品导电性的制约,无法直接观察黏土矿物的形貌特征,更无法真实地呈现黏土矿物表面纳米/亚纳米尺度的结构特征。超分辨光学显微术主要通过可见光振幅的变化或偏振光的干涉对矿物表面的微形貌进行观察,前人利用该方法观察到绿柱石、金刚石、磁铁矿、黄铁矿、闪锌矿、沸石等矿物表面的螺旋位错结构,揭示了矿物形貌与生长机理间的关系,推动了矿物生长理论的发展。但是该方法观察对象局限在解理面这类平坦表面,无法对粗糙、凹凸不平的表面进行观察^[6-14]。所以电子显微术与超分辨光学显微术在黏土矿物形貌精细表征与定量分析研究中存在一定的缺陷。原子力显微镜(AFM)作为第三代扫描探针显微镜,在纵、横向具有超高分辨率,不仅可同时观察矿物在二维平面与三维空间的形貌特征,还可对矿物形貌特征进行定量分析,是一种强有力的表面形貌观察手段。近年Gratz等^[13]利用AFM对石英表面的蚀像进行了精细表征,观察到纳米级的突缘与位错沟,证实了硅酸盐溶解和生长的突缘运动模型。Hochella等^[15]利用AFM观察到赤铁矿表面的波状起伏现象,揭示了矿物表面的断口效应。Friedbacher等^[16]和Jr Eggleston等^[17]和Johnson等^[18]分别利用AFM观察到Stultorum贝壳和钠长石表面形貌特征,揭示了晶体生长机制。上述研究成果促进了矿物表面纳米/亚纳米尺度形貌特征的研究,使矿物表面生长形貌特征的研究日趋精细化。而且,AFM方法克服了黏土矿物在层间交换性阳离子及离子力的作用下形成团聚体及单晶难以剥离的影响,可直接观察黏土矿物表面微形貌特征,从而揭示晶体表面纳米/亚纳米形貌及孔隙结构特征,因此,该方法近年被逐渐应用于非常规油气储层评价工作中^[19]。

川西须家河致密砂岩储层蕴藏了丰富的天然气资源,黏土矿物是该储层主要的组成矿物之一,随着勘探开发的深入,亟需对黏土矿物形貌进行精细表征。因此,本文以川西须家河组晚成岩阶段致密砂岩为研究对象,利用AFM分析技术研究黏土矿物中伊蒙混层、绿泥石与伊利石的形貌特征,揭示晶体表

面微形貌的指示意义、黏土矿物形貌特征与成岩作用间的关系,以及纳米孔隙的结构特征,从而为致密砂岩储层的评价提供科学依据。

1 实验部分

1.1 实验样品

实验样品为川西须家河致密砂岩,石英和长石含量较高,填隙物含量低,主要为胶结物,杂基含量少^[20],通过X射线衍射(XRD)分析,样品中黏土矿物主要为伊蒙混层黏土(占黏土总量的相对含量为76.2%)、绿泥石(占黏土总量的相对含量为21.2%)及少量伊利石(占黏土总量的相对含量为2.6%)。

1.2 样品制备

将致密砂岩粉碎至200目,按照《沉积岩中黏土矿物和常见非黏土矿物X射线衍射分析方法》(SY/T 5163—2018)进行黏土提取,将提取的黏土矿物配制成浓度为5%的溶液,滴于干净的载玻片,待自然风干后用于测试。

1.3 实验方法

实验采用Park NX10原子力显微镜,横向分辨率0.05nm,纵向分辨率0.015nm,扫描频率0.15~0.4Hz,阈值(Setpoint)为20nm,XY扫描范围100μm×100μm,Z扫描范围15μm。在原子力显微镜扫描过程中,由于黏土矿物局部仍然存在团聚现象,形成表面的异常凸起,因此参数的选择兼顾不同扫描区域下仪器的分辨率与黏土矿物团聚体的大小,避免扫描过程中污染纳米探针,从而影响图像质量。

2 结果与讨论

2.1 伊蒙混层黏土矿物的形貌特征

伊蒙混层黏土是川西须家河组主要的黏土矿物之一,是伊利石与蒙脱石两个端员矿物之间的过渡矿物,亦是成岩阶段划分的重要标志^[21]。本文利用原子力显微镜观察伊蒙混层黏土矿物晶体表面形貌特征(图1中a,b,c),根据晶体结晶位向差可知^[22],在1μm×1μm扫描区域存在两个晶界,将扫描区域分为三个晶粒(图1a),分别为图1a中的A、B、C,粒径在100~300nm之间,晶粒均由水平生长层在三维空间堆垛而层,晶棱间距整体上呈上疏下密的规律。而且从图1a-A中可明显观察到伊利石生长层在空间堆垛形成独特的“宝塔”形,伊利石与蒙脱石的晶棱局部呈溶蚀港湾状,而不是理想的面平棱直的晶体生长形态。此外,通过定量分析,晶粒上

部阶梯间距集中分布在 $\pm 0.6\text{nm}$ 、晶粒下部阶梯间距集中分布在 $0.3\sim 0.8\text{nm}$ (表1)。

伊蒙混层作为一常规与非常规油气储层中常见的混层黏土矿物,观察其形貌特征对于储层物理特性研究具有重要意义。前人利用电子显微术、超分辨光学显微术观察到伊蒙混层黏土矿物主要呈棉絮状包膜、薄膜状、柿壳状等形态特征,进而阐述了其晶面条纹的成因、晶体生长机制^[4,7,23]。本次研究利用原子力显微镜观察到晶体亚纳米生长层在二维平面的展布特征与三维空间的堆垛规律^[21]。根据伊蒙混层黏土形貌特征,结合晶体周期性键链(PBC)理论,在图1a-C中的晶面为伊蒙混层黏土矿物晶体生长层在三维空间堆垛形成的阶梯面(S面),该晶面与平坦面(F面)相邻,属于亚稳定状态的晶面,表明川西须家河组晚成岩阶段的伊蒙混层黏土矿物中伊利石与蒙脱石虽然是两种独立物相在二维平面紧密共生,但处于一个不稳定状态,再结合伊利石、蒙脱石晶体内部空间格子构造及晚成岩阶段伊利石、蒙脱石外部稳定赋存环境,可知该成岩阶段中伊蒙混层黏土中的两种黏土矿物处于一个动态转化过程,该晶面在伊蒙混层黏土中较发育,形成了大量的纳米孔隙,是致密砂岩中主要的纳米级储集空间。在伊利石生长过程中,由于晶面生长向外平行推移,在图1a中A、B形成了砂钟状构造,结合科赛尔-斯

特兰斯基层生长理论,说明伊利石生长过程中物质浓度过饱和^[22-24]。但是,不论是伊利石晶体还是蒙脱石晶体,其晶棱局部均呈溶蚀港湾状,而不是理想的面平棱直的晶体生长终态,表明晶体在生长过程中物质浓度发生了轻微的变化,导致晶棱出现不同程度的溶蚀,使得局部呈溶蚀港湾状。此外,伊蒙混层黏土矿物阶梯间距与单原子分子层厚度相当,表明伊蒙混层黏土矿物的基本结构单元为单原子层所组成,其生长机理是结晶微粒以晶核为中心二维附着生长并延展^[22]。

2.2 绿泥石矿物的形貌特征

绿泥石作为川西须家河组致密砂岩中一种主要的黏土矿物,通过原子力显微镜观察到绿泥石生长层主要有两种形态特征:一种是呈面平棱直的近正六边形理想晶体生长终态,且生长层在纵向上呈有规律的无隙叠置(图2中a,b,c);另一种呈不规则纺锤状,与近正六边形晶体生长层在纵向交互出现(图2a)。通过原子力显微镜的精细刻画,揭示了处于生长状态的绿泥石生长层由小到大向外平行推移生长,晶棱平直且互相平行。此外,通过定量分析,绿泥石晶体生长层单层厚度在 5nm 左右。

绿泥石为 $2:1$ 型的层状硅酸盐,它与伊蒙不同的是,其间是八面体氢氧化物片层^[20,25]。本次研究观察到的近正六边形绿泥石晶体生长层相较于扫

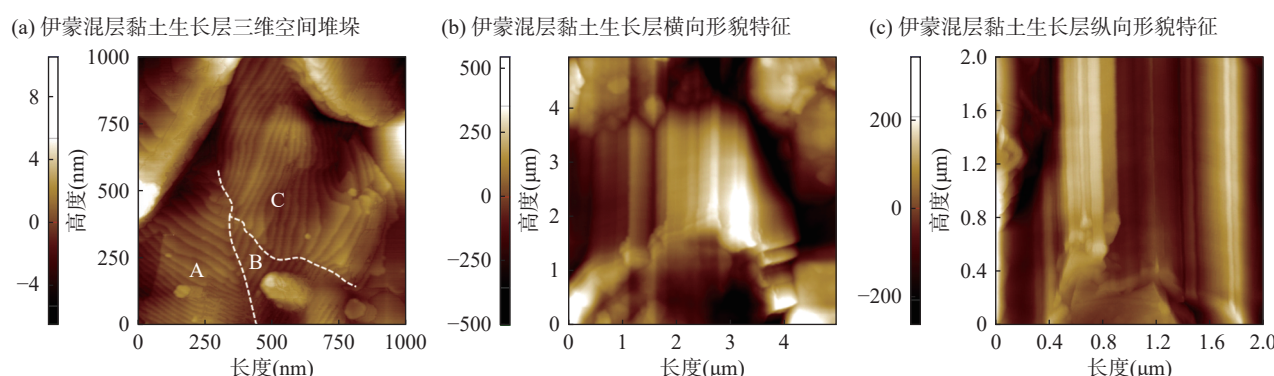


图1 伊蒙混层黏土矿物形貌特征

Fig. 1 Morphological characteristics of illite-smectite mixed-layer clay minerals: (a) Three-dimensional stacking of the growth layer; (b) Transverse morphology characteristics of the growth layer; (c) Longitudinal morphology characteristics of the growth layer.

表1 伊蒙混层黏土矿物阶梯高度

Table 1 Ladder height of illite-smectite mixed-layer clay minerals.

图例	阶梯高度 (nm)								
	图1a-A	图1a-B	图1a-C	图1a-D	图1a-E	图1a-F	图1a-G	图1a-H	
图1a-A	0.569	0.628	0.814	0.704	0.627	0.671	0.674	0.603	0.835
图1a-B	0.537	0.42	0.465	0.41	0.364	0.856	0.716	0.683	1.008
图1a-C	0.516	0.747	0.862	0.359	0.48	0.658	0.319	0.387	0.54

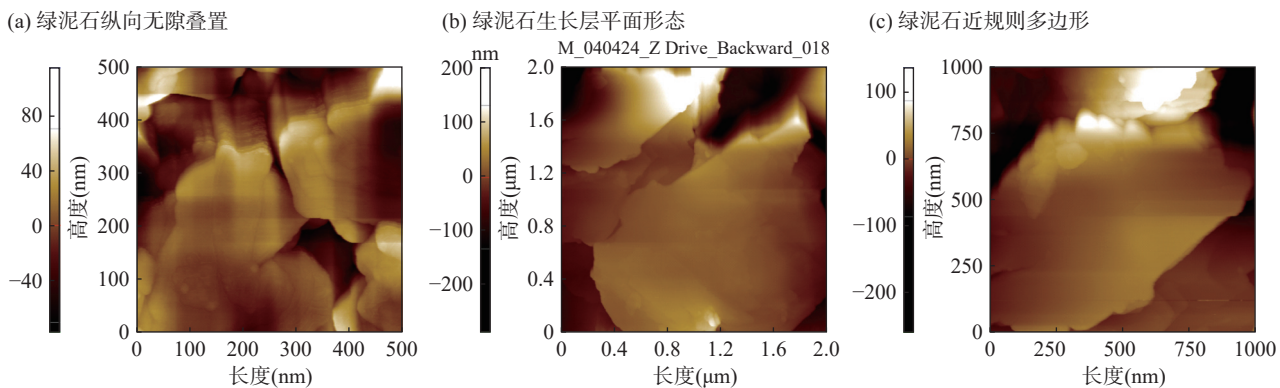


图2 绿泥石形貌特征

Fig. 2 Morphologic characteristics of chlorite: (a) Chlorite longitudinal no-gap superposition; (b) Plane morphology of chlorite growth layer; (c) Near-regular polygon of chlorite.

扫描电镜下观察到的叶片状和玫瑰花状，该生长层在纵向上无隙叠置，结合黏土矿物层间电荷的相关特性，表明绿泥石层间域含一定的层间阳离子，具有较强的吸附性，导致其纵向上层间缝隙不发育^[22-24]。根据绿泥石生长层形态特征，结合科赛尔-斯特兰斯基层生长理论，表明川西须家河晚成岩阶段绿泥石晶体生长处于过饱和且浓度稳定的生长环境。此外，通过定量分析绿泥石生长层厚度为单原子分子层厚度的5倍，结合晶体生长理论，表明川西须家河组晚成岩阶段绿泥石晶体处于过饱和的生长环境，但是由于生长过程中杂质原子被阶梯吸附，导致部分绿泥石生长层停止生长或生长速度减缓，形成生长层的重叠，从而使得绿泥石晶体的生长层变厚。

2.3 伊利石矿物的形貌特征

伊利石是一种富钾元素的二八面体黏土矿物，其晶体结构由2个四面体片夹一个八面体片构成，利用原子力显微镜在不同尺度分别对伊利石集合体

与晶体生长层形貌特征进行观察。在10μm×10μm大视域形貌图中，伊利石集合体形态不规则，边界局部被溶蚀呈港湾状，由于溶蚀作用在伊利石集合体边界处发育阶梯面(S)，集合体晶面局部可见伊利石鳞片状雏晶堆积(图4中a, b, c)。在1μm×1μm精细扫描图中，伊利石晶体生长层主要呈无定形态、表面平坦、平直晶棱与溶蚀港湾状晶棱间隔出现(图4中a, b, c)。此外，通过定量分析，伊利石生长层厚度在4~7nm。

伊利石作为川西须家河组致密砂岩晚成岩阶段一种主要的自生矿物，本次研究所观察到的伊利石晶体生长层的形态特征与扫描电镜下所观察到的刀片状、卷刃刀片状、薄膜状、丝缕状及蜂窝状有较大的差异^[26-33]。根据伊利石集合体表面的形貌特征，结合晶体层生长理论与晶体周期性键链(PBC)理论，表明该阶段伊利石处于亚稳定状态，但是该晶面发育的大量平行阶梯条纹或波纹状阶梯可为非常规储

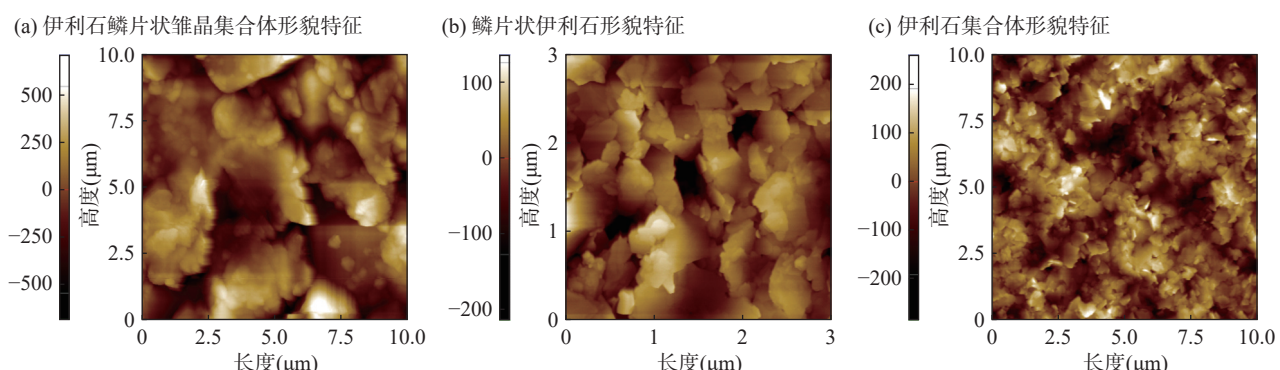


图3 在10μm×10μm大视域形貌图中伊利石矿物形貌特征

Fig. 3 Mineral morphologies of illite in 10μm×10μm large field of view: (a) Morphology characteristics of illite microcrystalline aggregate; (b) Morphology of scaly illite; (c) Morphological characteristics of illite aggregate.

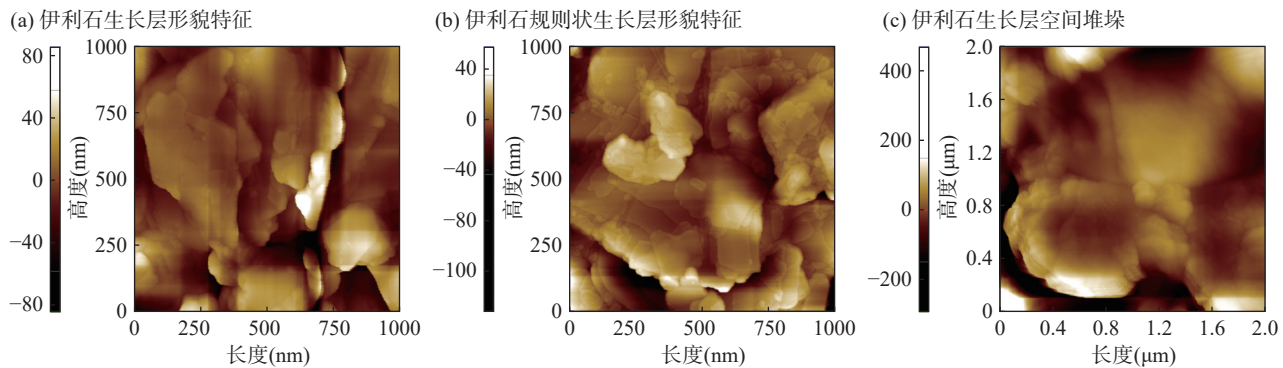


图4 在 $1\mu\text{m}\times 1\mu\text{m}$ 精细扫描图中伊利石矿物形貌特征

Fig. 4 Mineral morphologies of illite in $1\mu\text{m}\times 1\mu\text{m}$ fine scanning images: (a) Morphology of illite growth layer; (b) Morphology of illite regular growth layer; (c) Illite growth layer space stacking.

层提供大量的纳米孔隙。通过精细扫描揭示伊利石晶体生长层并不是“面平棱直”的生长终态,结合晶体层生长理论,表明伊利石晶体生长层处于不稳定的生长状态^[22-24]。此外,通过定量分析伊利石生长层厚度为单原子分子层厚度的5倍,结合晶体生长理论,表明川西须家河组晚成岩阶段伊利石晶体生长层生长过程中杂质原子被阶梯吸附,致使部分伊利石生长层停止生长或生长速度减缓,形成生长层的重叠,从而使得伊利石晶体生长层变厚。

3 结论

利用原子力显微镜揭示了川西须家河组致密砂岩储层中黏土矿物的纳米/亚纳米形貌特征,利用原子力显微镜超高空间分辨率优势观察到伊蒙混层黏土矿物主要发育平行阶梯条纹,其表面发育的阶梯面(S面);伊利石作为主要的黏土矿物之一,晶面平坦光滑,纵向上发育生长层平行阶梯条纹及波纹状

阶梯,是纳米孔隙发育的主要载体矿物;绿泥石形态规则,在纵向上无隙叠置。通过定量分析,伊利石与伊蒙混层生长层是单原子层构成,绿泥石生长层为多原子分子层所构成,揭示了同一成岩阶段不同黏土矿物生长层厚的差异,从而为非常规油气储层与黏土矿物形貌特征与成岩作用之间的耦合关系的研究提供微观依据。

利用原子力显微镜观察黏土矿物表面微形貌特征,解决了电子显微术前处理过程中金属离子对纳米形貌特征的“二次改造”,真实地呈现了黏土矿物生长层二维/三维空间形貌特征;同时亦克服了黏土矿物层间阳离子静电吸附的影响,精细表征了生长层纵横向的展布特点。为了更加系统地研究矿物亚纳米-纳米结构特征,该方法需与其他微区分析方法相结合,从而更加有力地支撑亚纳米-纳米矿物学的发展。

The Morphological Characteristics of Clay Minerals in a Tight Sandstone Reservoir by Atomic Force Microscopy

WANG Kunyang, DU Gu*, WANG Guan, HE Jiale

(Chengdu Center, China Geological Survey, Chengdu 610081, China)

HIGHLIGHTS

- (1) Atomic force microscopy (AFM) overcomes the influence of surface charge of clay minerals and accurately characterizes the surface nanometer/sub-nanometer morphology of clay minerals, which is an effective method for micro-region morphology observation.
- (2) Crystal surface steps were developed on the surface of clay minerals in Xujiahe tight sandstone in western Sichuan, which were the main component of nanopores.
- (3) The thickness of different clay mineral growth layers in the same diagenetic stage was different, and there was a spatial coupling relationship with diagenetic processes.

ABSTRACT: Clay minerals, as one of the main components of unconventional oil and gas reservoirs, have significant implications for the evaluation of unconventional oil and gas reservoirs in terms of their fine characterization of nano/sub-nano morphological features. By using atomic force microscopy (AFM) micro-area analysis technology, the problem of secondary modification of nano-pore structure caused by the conductive film in the pretreatment process of electron microscopy was solved; it made up for the defect that electron microscopy requires the sample to be conductive and can directly observe the morphological characteristics of the sample. Here, it was observed through AFM, that in the late diagenetic stage of the tight sandstone of the Xujiahe Formation in western Sichuan, some clay minerals developed parallel stepped stripes, with a large number of nano-pores formed at the concave angles on both sides of the steps, which were the main components of inorganic pores. Secondly, clay minerals had the same diagenetic evolution sequence, but their crystal morphologies were different, indicating that there was a spatial coupling relationship between their morphological features and diagenesis. The BRIEF REPORT is available for this paper at <http://www.ykcs.ac.cn/en/article/doi/10.15898/j.ykcs.202404040075>.

KEY WORDS: atomic force microscopy; tight sandstone; illite-smectite mixed-layer clay minerals; chlorite; illite; growth ladder; Xujiahe Formation in western Sichuan

BRIEF REPORT

Significance: Tight sandstone gas, as an important part of unconventional oil and gas resources, is the main substitute for conventional oil and gas resources. The study of mineralogical characteristics of tight sandstone reservoirs has always been a hot spot in the field of unconventional oil and gas. Clay minerals are one of the main constituent minerals of tight sandstone reservoirs. Focusing on the morphological characteristics of clay minerals cannot only establish a correspondence between different stages of sedimentary rock formation and the morphological characteristics of clay minerals, but can also trace the influence of temperature, impurities, and atomic behavior on the micro-morphological features of crystals during crystal growth, providing a basis for research on sedimentary environments and reservoir evaluation, with significant research significance. Here, the fine characterization of the etch image of a quartz surface was carried out using AFM, revealing nanoscale rims, dislocation grooves, shells, and sub-nanometer/nanometer-scale morphological features of feldspar surfaces. This work confirms the edge migration model of silicate dissolution and growth and reveals the mechanism of crystal growth.

Methods: The sample is a core of a tight sandstone reservoir from the Xiujahe Formation in western Sichuan. The sample was crushed to 200 mesh, and clay minerals were extracted according to the standard *Analysis Method for Clay Minerals and Ordinary Non-Clay Minerals in Sedimentary Rocks by the X-Ray Diffraction* (SY/T 5163—2018). The extracted clay minerals were prepared into a 5% solution and dropped onto a clean glass slide. After natural air drying, the slide was used for testing. The testing was performed using a Park NX10 atomic force microscope, with the following parameters set: scanning frequency of 0.15Hz to 0.4Hz, threshold (Setpoint) of 20nm, XY scanning range of 100μm×100μm, and Z scanning range of 15μm.

Data and Results: The surface morphology of illite-smectite mixed-layer clay minerals was observed using atomic force microscopy. Based on the crystal orientation difference, it was found that there were two grain boundaries in the 1μm×1μm scanning area, dividing the scanning area into three grains with a size of 100 to 300nm. The grains were formed by the stacking of horizontal growth layers in three-dimensional space, and the spacing of the crystal edges showed an overall pattern of being denser at the bottom and sparser at the top. The growth layers of illite formed a unique “pagoda” shape when stacked in space, and the crystal edges of illite and smectite were locally eroded in a bay-like shape rather than the ideal flat and straight crystal growth end state. Additionally, through quantitative analysis, the step spacing at the upper part of the grains was concentrated at 0.6nm±, and the step spacing at the lower part of the grains was concentrated at 0.3 to 0.8nm. The growth layers of chlorite mainly had two morphological characteristics: one was the ideal flat and straight near-hexagonal crystal growth end state, and the growth layers were regularly stacked without gaps in the vertical direction; the other was an irregular spindle shape, which alternated with the near-hexagonal crystal growth layers in the vertical direction. Through the detailed characterization of atomic force microscopy, it was revealed that the growth layers of chlorite in the growth state were parallelly pushed outward from small to large, with straight and parallel crystal edges. Additionally, through quantitative analysis, the single-layer thickness of the chlorite crystal growth layers was approximately 5nm. The morphology of illite aggregates was irregular, with locally eroded boundaries in a bay-like shape. Due to the erosion, step faces (S) developed at the boundaries of the illite aggregates, and local illite flaky microcrystals were observed on the crystal faces of the aggregates. In the fine scan images, the growth layers of illite crystals were mainly amorphous, with flat surfaces, and straight and eroded bay-like crystal edges appearing alternately. Additionally, through quantitative analysis, the thickness of the illite growth layers was 4 to 7nm.

参考文献

- [1] 叶荣, 涂光炽, 马喆生, 等. 热液矿床矿物微形貌与晶体生长环境研究[J]. 地学前缘, 2005, 12(2): 240–246.
Ye R, Tu G Z, Ma Z S, et al. The surface micromorphology of minerals in hydrothermal ore deposits and growth environments of crystal[J]. *Earth Science Frontiers*, 2005, 12(2): 240–246.
- [2] 陈光远, 孙岱生. 成因矿物学找矿矿物学新进展[M]. 北京: 原子能出版社, 1998: 12–16.
Chen G Y, Sun D S. New development in genetic mineralogy and prospecting mineralogy[M]. Beijing: Atomic Energy Press, 1998: 12–16.
- [3] 陈光远, 鲁安怀. 矿物成分标型继承性与金矿矿质来源[J]. 地学前缘, 1994, 1(3–4): 204–209.
Chen G Y, Lu A H. Chemical inheritance of mineral typomorphism and source of gold[J]. *Earth Science Frontiers*, 1994, 1(3–4): 204–209.
- [4] 王坤阳, 杜谷. 利用原子力显微镜与能谱-扫描电镜研究页岩孔隙结构特征[J]. 岩矿测试, 2020, 39(6): 839–846.
Wang K Y, Du G. Study on the pore structure characteristics of shale by atomic force microscope and energy spectrum-scanning electron microscope[J]. *Rock and Mineral Analysis*, 2020, 39(6): 839–846.
- [5] 王羽, 汪丽华, 王建强, 等. 基于聚焦离子束-扫描电镜方法研究页岩有机孔三维结构[J]. 岩矿测试, 2018, 37(3): 235–243.
Wang Y, Wang L H, Wang J Q, et al. Three-dimension characterization of organic matter pore structures of shale using focused ion beam-scanning electron microscope[J]. *Rock and Mineral Analysis*, 2018, 37(3): 235–243.

- [6] 许谊, 徐毓娴, 惠梅, 等. 微分相干干涉显微镜定量测量表面形貌[J]. *光学精密工程*, 2001, 9(3): 227–230.
- Xu Y, Xu Y X, Hui M, et al. Quantitative surface topography determination by differential interference contrast microscopy[J]. *Optics and Precision Engineering*, 2001, 9(3): 227–230.
- [7] Barty A, Nugent K A, Paganin D, et al. Quantitative optical phase microscopy[J]. *Optics Letters*, 1998, 23(11): 817–819.
- Liao L B, Li S Z. Effect of SPM scanning range on the micromorphology parameters[J]. *International Journal of Minerals, Metallurgy and Materials*, 1995, 5(1): 36–38.
- [9] 戚明辉, 李君军, 曹茜. 基于扫描电镜和JMicroVision图像分析软件的泥页岩孔隙结构表征研究[J]. *岩矿测试*, 2019, 38(3): 260–269.
- Qi M H, Li J J, Cao Q. The pore structure characterization of shale based on scanning electron microscopy and JMicroVision[J]. *Rock and Mineral Analysis*, 2019, 38(3): 260–269.
- [10] 朱炎铭, 王阳, 陈尚斌, 等. 页岩储层孔隙结构多尺度定性-定量综合表征: 以上扬子海相龙马溪组为例[J]. *地学前缘*, 2016, 23(1): 154–163.
- Zhu Y M, Wang Y, Chen S B, et al. Qualitative-quantitative multiscale characterization of pore structures in shale reservoirs: A case study of Longmaxi Formation in the upper Yangze area[J]. *Earth Science Frontiers*, 2016, 23(1): 154–163.
- [11] Klaver J, Desbois G, Urai J L, et al. BIB-SEM study of the pore space morphology in early mature Posidonia shale from the Hils area, Germany[J]. *International Journal of Coal Geology*, 2012, 103: 12–25.
- [12] 黄振凯, 陈建平, 王义军, 等. 微米CT在烃源岩微观结构表征方面的应用[J]. *石油实验地质*, 2016, 38(3): 418–422.
- Huang Z K, Chen J P, Wang Y J, et al. Application of micron CT in the characterization of microstructure in source rocks[J]. *Petroleum Geology & Experiment*, 2016, 38(3): 418–422.
- [13] Gratz A J, Hillner P E. Poisoning of calcite crystal growth viewed in the atomic force microscope (AFM)[J]. *Journal of Crystal Growth*, 1993, 129(3): 789–793.
- [14] 姚素平, 焦堃, 张科, 等. 煤纳米孔隙结构的原子力显微镜研究[J]. *科学通报*, 2011, 56(22): 1820–1827.
- Yao S P, Jiao K, Zhang K, et al. An atomic force microscopy study of coal nanopore structure[J]. *Chinese Science Bulletin*, 2011, 56(22): 1820–1827.
- [15] Hochella M F, Jr Eggleston C M, Elings V B, et al. Mineralogy in two dimensions: Scanning tunneling microscopy of semiconducting minerals with implications for geochemical reactivity[J]. *American Mineralogist*, 1989, 74: 1233–1246.
- Friedbacher G, Hansma P K. Imaging powders with the atomic force microscope: From biominerals to commercial materials[J]. *Science*, 1991, 253: 1261–1262.
- Jr Eggleston C M, Hochella M F. Scanning tunneling microscope of sulfide surface[J]. *Geochimica et Cosmochimica Acta*, 1990, 54: 1551–1517.
- Johnson P D, Eggleston C M, Hochella M F. Imaging molecular-scale structure and microtopography of hematite with the atomic force microscope[J]. *American Mineralogist*, 1991, 76: 1442–1445.
- [19] 廖立兵, 马皓生, 施倪承. 扫描隧道显微镜和原子力显微镜在矿物学研究中的应用现状及前景[J]. *现代地质*, 1993, 7(4): 5.
- Liao L B, Ma Z S, Shi N C. Application status and prospect of scanning tunneling microscope and atomic force microscope in mineralogy research[J]. *Geoscience*, 1993, 7(4): 5.
- [20] 孙全力, 孙晗森, 贾昀, 等. 川西须家河组致密砂岩储层绿泥石成因及其优质储层关系[J]. *石油与天然气地质*, 2012, 33(5): 751–757.
- Sun Q L, Sun H S, Jia B, et al. Genesis of chlorite in tight sandstone reservoirs of Xujiahe Formation in western Sichuan and its relationship with high-quality reservoirs[J]. *Oil & Gas Geology*, 2012, 33(5): 751–757.
- [21] 周张健. 蒙脱石伊利石化的控制因素、转化机制及其转化模型的研究综述[J]. *地质科技情报*, 1994, 13(4): 41–46.
- Zhou Z J. Review on control factors, transformation mechanism and transformation model of montmorillonite illization[J]. *Geological Science and Technology Bulletin*, 1994, 13(4): 41–46.
- [22] 李胜荣, 许虹, 申俊峰, 等. 结晶学与矿物学[M]. 北京: 地质出版社, 2008: 9–18.
- Li S R, Xu H, Shen J F, et al. *Crystallography and mineralogy*[M]. Beijing: Geological Publishing House, 2008: 9–18.
- [23] 潘兆橹. 结晶学及矿物学[M]. 北京: 地质出版社, 1993: 15–26.
- Pan Z L. *Crystallography and mineralogy* [M]. Beijing: Geological Publishing House, 1993: 15–26.
- [24] 王文魁, 王继扬, 赵珊茸, 等. 晶体形貌学[M]. 北京: 中国地质大学出版社, 2001: 22–27.
- Wang W K, Wang J Y, Zhao S R, et al. *Crystal morphology*[M]. Beijing: China University of

- Geosciences Press, 2001: 22–27.
- [25] 张天乐, 王宗良. 中国粘土矿物的电子显微研究 [M]. 北京: 地质出版社, 1978: 33–41.
Zhang T L, Wang Z L. Electron microscopy of clay minerals in China [M]. Beijing: Geological Publishing House, 1978: 33–41.
- [26] 徐春华, 朱光, 刘国生, 等. 伊利石结晶度在恢复地层剥蚀量中的应用—伊利石结晶度在恢复地层剥蚀量中的应用——以合肥盆地安参1井白垩系剥蚀量的恢复为例 [J]. 地质科技情报, 2005, 24(1): 41–44.
Xu C H, Zhu G, Liu G S, et al. Application of crystallinity of illite to recover denudation quantity: An example of Cretaceous denudation quantity recovery of Well Ancan 1 in Hefei Basin, Anhui Province [J]. Geological Science and Technology, 2005, 24(1): 41–44.
- [27] 张有瑜, 罗修全. 油气储层自生伊利石 K-Ar 同位素年代学研究现状与展望 [J]. 石油与天然气地质, 2004, 25(2): 231–236.
Zhang Y Y, Luo X Q. K-Ar isotopic chronological study of authigenic illite in reservoirs [J]. Oil & Gas Geology, 2004, 25(2): 231–236.
- [28] 达比 D. 伊利石年龄记录着石油盆地中深部流体运动 [J]. 地质科技动态, 1998(9): 8–13.
Da B. Illite age records deep fluid movement in petroleum basin [J]. Geological Science and Technology Trends, 1998(9): 8–13.
- [29] 车忱, 杨忠芳, 季峻峰. 沉积岩中成岩伊利石年龄测定研究进展 [J]. 地球科学进展, 2002, 17(5): 693–698.
Che C, Yang Z F, Ji J F. Research progress in dating of authigenic illite in sedimentary [J]. Advance in Earth Science, 2002, 17(5): 693–698.
- [30] 杨瑞, 田元, 李晓波, 等. 章村伊利石矿中主要粘土矿物的微观形貌特征及成因分析 [J]. 地球科学前沿, 2020, 10(2): 7.
Yang R, Tian Y, Li X B, et al. Micromorphologic characteristics and genetic analysis of main clay minerals in Zhangcun illite mine [J]. Earth Science Frontiers, 2020, 10(2): 7.
- [31] 刘钰洋, 潘懋, 刘诗琦, 等. 鄂尔多斯盆地白于山井网加密区延长组长 4+5 特低渗储层沉积特征和储层物性分析 [J]. 北京大学学报 (自然科学版), 2018, 54(5): 1028–1039.
Liu Y Y, Pan M, Liu S Q, et al. Comprehensive depositional system and reservoir characterization study of Chang 4+5 reservoir of Yanchang Group, infill well region in Baiyushan area, Ordos Basin [J]. Acta Scientiarum Naturalium Universitatis Pekinensis, 2018, 54(5): 1028–1039.
- [32] Ahn J H, Peacor D R. Transmission and analytical electron microscopy of the smectite to illite transition [J]. Clay and Clay Minerals, 1986, 34(2): 165–179.
- [33] 李嵘, 吕正祥, 叶素娟. 川西拗陷须家河组致密砂岩成岩作用特征及其对储层的影响 [J]. 成都理工大学学报 (自然科学版), 2011, 38(2): 147–155.
Li R, Lyu Z X, Ye S J. Impact of diagenesis on reservoir-quality evolution in the upper Triassic Xujiahe tight sandstones, West Sichuan, China [J]. Journal of Chengdu University of Technology (Natural Science Edition), 2011, 38(2): 147–155.